Molecular Medicine

Supplemental Data

CSE1L, a Novel Microvesicle Membrane Protein, Mediates Ras-Triggered Microvesicle Generation and Metastasis of Tumor Cells

Ching-Fong Liao,[1] Shu-Hui Lin,[2,3*] Hung-Chang Chen,[4] Cheng-Jeng Tai,[5,6] Chun-Chao Chang,[5,7] Li-Tzu Li,[1] Chung-Min Yeh,[2,3] Kun-Tu Yeh,[2,8,9] Ying-Chun Chen,[1] Tsu-Han Hsu,[1] Shing-Chuan Shen,[10] Woan-Ruoh Lee,[10] Jeng-Fong Chiou,[11] Shue-Fen Luo,[12] and Ming-Chung Jiang[5]*

Online address: http://www.molmed.org

The Feinstein Institute for Medical Research North Shore LIJ

Supplementary Table S1. Baseline characteristics of the colorectal cancer patients

Clinicopathological parameter	Stage I (N=13)	Stage II (N=43)	Stage III (N=43)	Stage IV (N=16)
Mean age (range), year[a]	66.0 ± 11.5, 42-84	65.4 ± 10.0, 40-93	60.3 ± 15.2, 28-92	71.1 ± 11.2, 46-87
Sex				
Male	7	27	27	7
Female	6	16	16	9
Tumor grade[b]				
Grade 1	0	0	2	2
Grade 2	13	41	39	14
Grade 3	0	1	3	0
Lymph node (N[c]) and distant metastasis (M[d])				
N0M0	13	43	0	0
N1M0	0	0	23	0
N2M0	0	0	20	0
N0M1	0	0	0	1
N1M1	0	0	0	15
N2M1	0	0	0	0

[a]Mean ± SD. [b]Grade 1: well differentiation, Grade 2: moderate differentiation, Grade 3: poor differentiation. [c]N0: no regional lymph node metastasis, N1: metastasis in 1-3 regional lymph nodes, N2: metastasis in ≥ 4 regional lymph nodes, [d]M0: no distant metastasis, M1: distant metastasis.

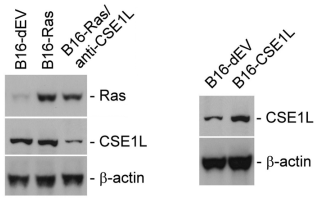

Supplementary Figure S1. Immunoblot analyses of the levels of Ras and CSE1L in B16-dEV, B16-Ras, B16-CSE1L, and B16-Ras/anti-CSE1L cells. The levels of Ras and CSE1L in cell lysates prepared from B16-dEV, B16-Ras, B16-CSE1L, and B16-Ras/anti-CSE1L cells were analyzed by immunoblot with anti-CSE1L (clone 24) and anti-Ras antibodies. β-actin levels were assayed as a control.

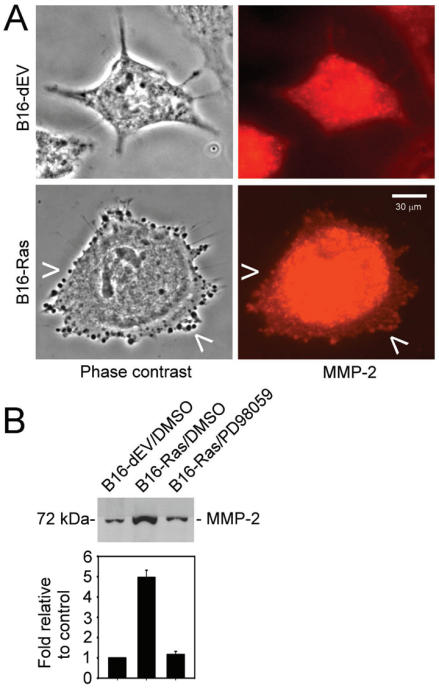

Supplementary Figure S2. v-H-ras transfection increased microvesicular MMP-2 level. (A) Immunofluorescence analysis of MMP-2 distribution in B16-dEV and B16-Ras cells with anti-MMP-2 antibodies. Note that microvesicles were rich in MMP-2 (arrowhead) in B16-Ras cells. Scale bar, 30 μm. (B) Levels of microvesicular MMP-2 in microvesicles harvested from cell number-standardized conditioned media from serum-starved B16-dEV and B16-Ras cells that treated with DMSO or 50 μM PD98059 for 48 h. Band intensities were quantified by densitometry, and the fold relative to control is shown.

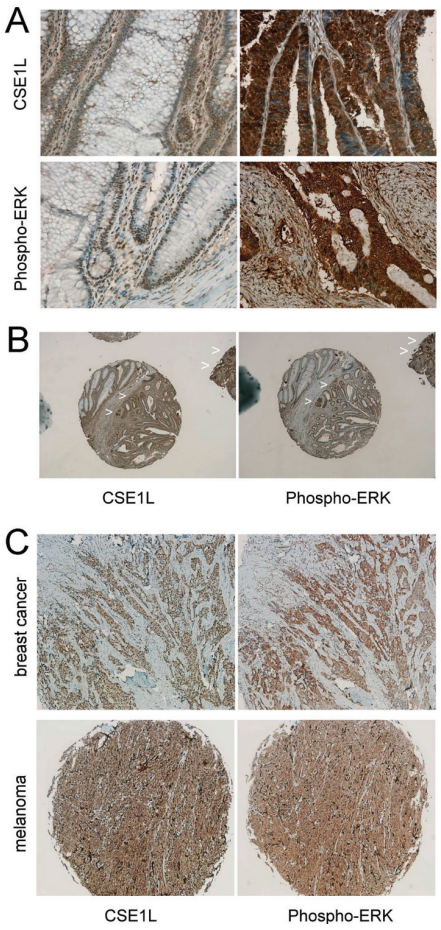

Supplementary Figure S3. Coincidence in the relative staining intensity of CSE1L with phospho-ERK in colorectal cancer, breast cancer, and melanoma. (A) Representative images show the expression of CSE1L and phospho-ERK in colorectal cancer analyzed by immunohistochemistry with tissue microarray consists of 115 cancer specimens. Left panels: non-tumor tissues; right panels: colorectal tumors. Original magnification: 400×. (B) Representative images of the relative staining intensity of CSE1L and phospho-ERK in tumors analyzed by immunohistochemistry with adjacent serial colorectal cancer tissue sections. Arrowheads indicate coincidence in the relative staining intensity of CSE1L with phospho-ERK in tumors. Original magnification: 40×. (C) Representative images of the relative staining intensity of CSE1L and phospho-ERK in tumors analyzed by immunohistochemistry with adjacent serial breast cancer and melanoma tissue sections. Original magnification: 40×.

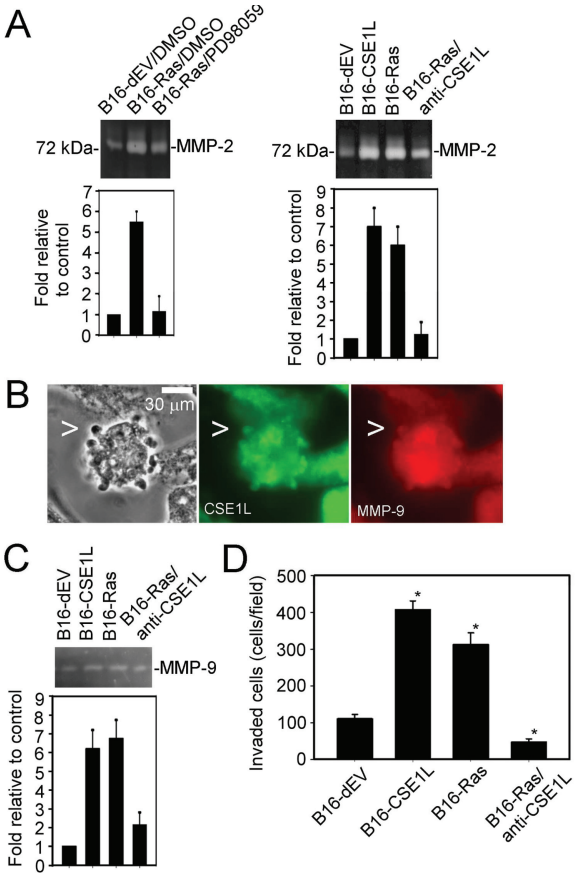

Supplementary Figure S4. CSE1L mediates the *in vitro* invasion of tumor cells induced by v-H-ras. (A) The gelatin zymographic activities of microvesicular MMP-2 in microvesicles harvested form the cell number-standardized conditioned media of serum-starved B16-dEV, B16-Ras, B16-CSE1L, and B16-Ras/anti-CSE1L cells treated with or without DMSO or 50 μM PD98059 for 48 h as indicated. Band intensities were quantified by densitometry, and the folds relative to control are shown. (B) Representative images show colocalization of CSE1L with MMP-9 in microvesicles analyzed by immunofluorescence with anti-CSE1L and anti-MMP-9 antibodies. (C) The gelatin zymographic activities of microvesicular MMP-9 in microvesicles harvested form the cell number-standardized conditioned media of serum-starved B16-dEV, B16-Ras, B16-CSE1L, and B16-Ras/anti-CSE1L cells. Band intensities were quantified by densitometry, and the folds relative to control are shown. (D) The *in vitro* invasion abilities of B16-dEV, B16-CSE1L, B16-Ras, and B16-Ras/anti-CSE1L cells analyzed by Matrigel-based invasion assays. The mean ± SD numbers of invasive cells were 109.4 ± 12.6, 406.8 ± 23.9, 311.25 ± 32.4, and 46.75 ± 8.7 cells per field for B16-dEV, B16-CSE1L, B16-Ras, and B16-Ras/anti-CSE1L cells, respectively. $P<0.0001$ between B16-CSE1L and B16-dEV cells. $P<0.0001$ between B16-Ras and B16-dEV cells. $P<0.0001$ between B16-Ras/anti-CSE1L and B16-dEV cells. $P<0.0001$ between B16-Ras and B16-Ras/anti-CSE1L cells.